HTML ABSTRACT • LINKS

Multiple relaxation mechanisms in $SrTiO_3/SrRuO_3$ heterostructures

Z.-G. Ban and S. P. Alpay[a)]
Department of Metallurgy and Materials Engineering and Institute of Materials Science, University of Connecticut, Storrs, Connecticut 06269

Feizhou He and B. O. Wells
Department of Physics, University of Connecticut, Storrs, Connecticut 06269

X. X. Xi
Department of Physics, The Pennsylvania State University, University Park, Pennsylvania 16802

(Received 24 November 2003; accepted 16 April 2004; published online 25 May 2004)

We have studied stress relaxation mechanisms in epitaxial (001) $SrTiO_3$ films grown on (001) $LaAlO_3$ substrates with $SrRuO_3$ buffer layers. A theoretical analysis has been undertaken to understand the variation of the lattice parameters of $SrTiO_3$ epitaxial films, taking into account stress relaxation due to the formation of an orthorhombic polydomain structure in the $SrRuO_3$ buffer layer as well as the formation of misfit dislocations at the $LaAlO_3/SrRuO_3$ and the $SrTiO_3/SrRuO_3$ interfaces. There exists a critical $SrRuO_3$ buffer layer thickness, above which the $SrRuO_3$ buffer layer can "screen" the effect of the $LaAlO_3$ substrate. It is shown that the internal stress level in films can be controlled using buffer layers that exhibit a structural phase transformation. © *2004 American Institute of Physics.* [DOI: 10.1063/1.1760228]

In recent years, there is a growing interest in perovskite thin films due to their unique electrical, electromechanical, and magnetic properties. Perovskite oxides in thin film form exhibit remarkably different physical properties compared to their bulk counterparts due to compositional and microstructural inhomogeneities, defects, and internal stresses.[1] For epitaxial perovskite thin films, the mismatch between the lattice parameters and thermal expansion coefficients of the film and the substrate are the predominant sources of the internal stresses.

In thin films, the internal stress state may become more complicated by the deposition of buffer layer(s) between the film and substrate. It has become common to use buffer layers both to promote proper epitaxy and to provide layers with appropriate properties for device applications. A good example of such a system is $SrTiO_3$ (STO) thin films grown on relatively thick substrates. STO is an ideal candidate for tunable microwave device applications.[2] Among a variety of electrode materials for STO films, $SrRuO_3$ (SRO) has received considerable interest due to its high electric conductivity, good thermal conductivity and stability, and high resistance to chemical corrosion.[3] Upon cooling, bulk SRO undergoes a first order cubic↔tetragonal (CT) transformation at 677 °C and subsequently a second-order tetragonal↔orthorhombic (TO) transformation at 547 °C.[4] If these transformations occur in an epitaxial film of SRO, the total elastic energy due to the self-strain of the phase transformation may be reduced by polydomain (polytwin) formation. The polydomain structure consists of elastic domains and their formation is a generic stress relaxation mechanism in a constraining media.[5] The parameters of polydomain structures and the conditions for their formation were quantitatively determined for epitaxial ferroelectric films undergoing CT and TO phase transformations.[5] It was shown that the resultant polydomain structure is due to the interplay between relaxation by misfit dislocations during film deposition and relaxation by polydomain formation below the phase transformation temperature.

This letter gives a quantitative theoretical analysis of the multiple stress relaxation mechanisms in STO epitaxial films grown on $LaAlO_3$ (LAO) substrates with SRO as buffer layers. The model used here considers first stress relaxation in the buffer layer with respect to the substrate and then treats the buffer layer/substrate combination as an effective substrate for the STO film. The theoretical predictions are used to interpret experimental observations. The trends predicted for film parameters as a function of both STO film thickness and buffer layer thickness are observed experimentally.

(001) STO films were grown on (001) LAO single-crystal substrates with (001) SRO buffer layers using pulsed laser deposition (PLD). The samples had either a variation in the STO layer thickness (50–1000 nm) or the SRO layer thickness (0–350 nm). The details of the PLD processing were reported elsewhere.[6] Good epitaxy was achieved with average mosaics around 0.2° detected using x-ray diffraction (XRD). XRD measurements were carried out at beamline X22A at the National Synchrotron Light Source at Brookhaven National Laboratory. X22A has a bent Si (111) monochromator, giving a small beam spot and fixed incident photon energy of 10 keV. The longitudinal resolution with a Si (111) analyzer was at least 0.001 $Å^{-1}$ (half width at half-maximum) for an (002) peak, as measured from the LAO substrates.

We have analyzed the CT and TO transformations in SRO using the theoretical formalism developed previously.[5] The relaxation of internal stresses at the deposition temperature (T_G = 720 °C) was taken into account using the effective substrate lattice parameter concept, assuming that no additional dislocations form during cooling down from T_G. The

[a)]Author to whom correspondence should be addressed; electronic mail: p.alpay@mail.ims.uconn.edu

 © 2004 American Institute of Physics

"effective" substrate lattice parameter $\bar{a}_S$ at a particular temperature T is given by:[7]

$$\bar{a}_S(T)=\frac{a_S^0[1+\kappa_S(T-T_G)]}{\rho(T_G)a_S^0[1+\kappa_S(T-T_G)]+1}, \quad (1)$$

where

$$\rho(T_G)\cong\frac{x_M(T_G)}{a_f^0}\left(1-\frac{h_\rho}{h_f}\right), \quad (2)$$

is the equilibrium linear dislocation density at the deposition temperature, h_f is the thickness of the SRO layer, a_S^0 and a_f^0 are the lattice parameters of the $LaAlO_3$ (LAO) substrate and SRO film (in the pseudocubic notation) at T_G, κ_S is the thermal expansion coefficient (TEC) of the substrate, $x_M(T_G)$ is the misfit strain between LAO and SRO at T_G, and h_ρ is the critical thickness for dislocation generation. h_ρ is around 4 nm for SRO on LAO, calculated from the Matthews–Blakeslee criteria.[8] The effective misfit strain at a particular temperature $x_M^*(T)$, therefore, can be determined by $\bar{a}_S(T)$ and $a_f(T)$. $a_f(T)$ is correlated with a_f^0 and the TEC of the film κ_f.

As the film cools down from $T_G=720\,°C$ to just below 600 °C, biaxial *tensile* stresses results within the SRO layer due to the mismatch in TECs of SRO and LAO. The tensile stresses should lead to the formation of an orthorhombic polydomain structure from the tetragonal c domain. Orthorhombic twins in epitaxial SRO thin films have been reported in several studies.[9–12] Just before the TO transformation, the SRO film consists of only c domains, and thus there are only two orthorhombic orientation variants (out of the possible six) that form the polydomain structure, identical to the $a_1/a_2/a_1/a_2$ polydomain pattern in twinned tetragonal films.[5,13] Theoretical results show that the fractions of the domains in this pattern are equal to each other.[5] The orientational relation between the two variants of the orthorhombic phase and the substrate is [001] SRO//[001] LAO and [100] SRO//[110] LAO.

The orthorhombic twin structure in the SRO layer was verified by the reciprocal space x-ray mapping of the in-plane lattice of STO and SRO layer at room temperature (Fig. 1). The film thickness of STO and SRO layer are 200 and 350 nm, respectively. We can clearly see (406) and (046) peaks from two SRO domains, as well as the STO (223) peak. Since the fractions of the domains of the orthorhombic phase are roughly identical, the in-plane lattice parameter of SRO can be taken as the average of the lattice parameters of the two orthorhombic variants, i.e., $1/2(a_{SRO}+b_{SRO})$.

We first examined the in-plane and out-of-plane lattice parameters of STO films of varying film thickness and the thickness of the SRO layer fixed at 350 nm at room temperature. Figure 2(a) presents the experimentally determined values and both in-plane parameters a_1 and a_2 were measured and differ due to experimental uncertainty. It shows that tensile stresses in STO layer are relaxed almost completely with increasing STO film thickness. We performed theoretical analysis based on the stress relaxation due to both the orthorhombic twin structure in the SRO layer and formation of misfit strain dislocations at the LAO/SRO and SRO/STO interfaces. The effective substrate lattice parameter concept

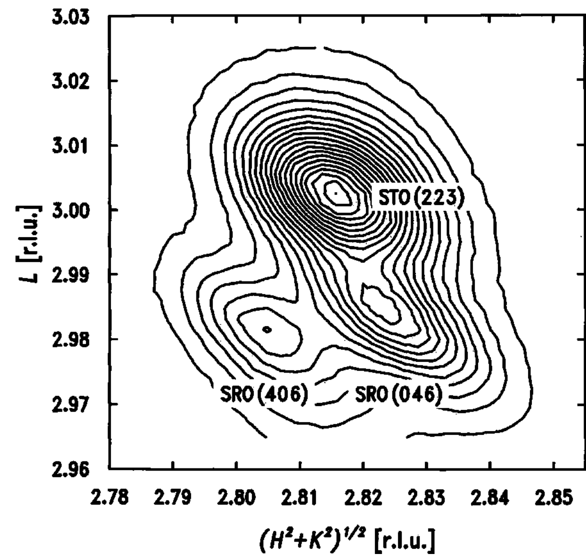

FIG. 1. Reciprocal space mapping of STO (223)/SRO (406) peaks at room temperature. The film thickness of STO and SRO layers are 200 and 350 nm, respectively. The upper peak is from STO (223) while the lower two are SRO (406)/(046) from two domains. The unit is in STO reciprocal lattice parameter.

[Eqs. (1)–(2)] is employed for both interfaces. The in-plane lattice constant of STO film a_{STO} is taken as the effective lattice parameter of the SRO layer and the out-of-plane lattice constant of STO film c_{STO} is given by:[14]

$$c_{STO}=a_{STO}\left(1-\frac{2C_{12}}{C_{11}}x_M^*\right), \quad (3)$$

where C_{ij} are the elastic moduli of STO and x_M^* is the in-plane misfit strain taking into account the relaxation by the misfit dislocation formation at STO/SRO interface. The calculated average distance between misfit dislocations at STO/

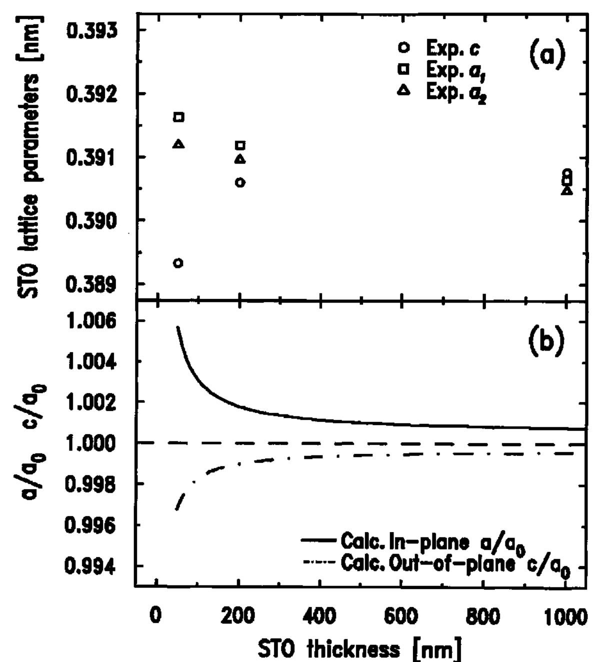

FIG. 2. Lattice parameters of STO films as a function of STO film thickness at room temperature: (a) experimentally determined in-plane (a_1 and a_2) and out-of-plane (c) lattice parameter; (b) theoretically calculated in-plane (solid line), and out-of-plane (dotted dashed line) lattice parameters.

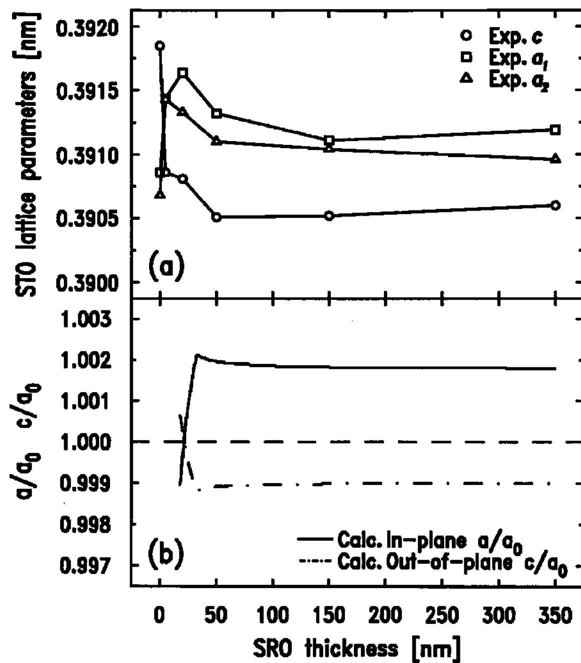

FIG. 3. Lattice parameters of 200 nm thick STO films as a function of SRO film thickness at room temperature: (a) experimentally determined in-plane (a_1 and a_2) and out-of-plane (c) lattice parameter; (b) theoretically calculated in-plane (solid line) and out-of-plane (dotted dashed line) lattice parameters.

SRO interface is on the order of 10^3 nm which yields a relatively low dislocation density ($\sim 10^{-3}$ nm^{-1}). This prediction is in very good agreement of recent high resolution transmission electron microscopy studies of defect structures in STO/SRO bilayer films on LAO substrate which show there are no misfit dislocations at the submicron scale.[15] Substantial stress relaxation occurs when STO film thickness h_{STO} is below 200 nm and there is no significant change when STO is thick enough (e.g., $h_{STO}>800$ nm). The lattice parameters of STO films are normalized with respect to a reference state a_0 that may be larger than the bulk lattice parameter of STO (0.3905 nm). The enlargement of the unit cell has been widely observed in STO and has been attributed to nonequilibrium defects, such as oxygen vacancies, associated with the deposition methods and conditions.[16–19] The normalization of the lattice parameter of STO films can provide us a general trend independent of the reference state. With this consideration, the theoretical calculations [Fig. 2(b)] are in good agreement with the experimental data [Fig. 2(a)].

A very interesting finding is associated with the role of the SRO buffer layer in the internal stress condition of STO top layer. In Fig. 3, we plot both theoretically and experimentally determined lattice parameters of STO films as a function of SRO film thickness with the STO film thickness fixed at 200 nm at room temperature using the same theoretical approach. The analysis shows that the internal stresses in STO change from compression to tension at $h_{SRO}\cong 25$ nm [see Fig. 3(b)]. Below this film thickness, the LAO substrate has an overwhelming influence on the top STO layer. Considering the stress relaxation by misfit dislocation formation, since the lattice parameter of LAO is less than that of STO, in-plane compressive stresses result in STO layer. Above this critical STO thickness, the effect of the SRO buffer layer becomes increasingly pronounced. Since the lattice parameter of SRO is larger than that of STO, tensile stresses are expected in the STO layer. When the SRO layer thickness is larger than ~ 35 nm, the lattice parameters of the STO layer above become insensitive to thickness variation of the SRO layer due to the saturation of the stress relaxation. Thus the effect of the LAO substrate is completely "screened" for SRO layer thickness larger than ~ 35 nm. The theoretical prediction reflects the general trend observed experimentally, as shown in Fig. 3(a). The experimental results appear to indicate a crossover from compressive to tensile stress as well but it occurs for even thinner buffer layers. For a very thin buffer layer, the out-of-plane lattice parameter of STO film is larger than the in-plane lattice parameter and compressive stresses should result if the STO reference state has a lattice parameter larger than the bulk value. In both cases, the full effect of the buffer layer is complete for buffer layer thickness of 50 nm or greater, with only small changes beyond 35 nm. Notably, both theoretical analysis and experimental result essentially suggest a design strategy for the buffer layer, i.e., the buffer layer does not have to be very thick (>35 nm to minimize the effect of the substrate on the top film.

This material is based upon work supported by the National Science Foundation under Grant No. DMR-0132918 (Z-G.B. and S.P.A.), DMR-0239667 (F.H. and B.O.W.) and DMR-9702632 (X.X.X.). F.H. and B.O.W. also acknowledge support from the Cottrell Scholars Program of the Research Corporation.

[1] T. M. Shaw, S. Trolier-McKinstry, and P. C. McIntyre, Annu. Rev. Mater. Sci. **30**, 263 (2000).
[2] X. X. Xi, H. C. Li, W. Si, A. A. Sirenko, I. A. Akimov, J. R. Fox, and A. M. Clark, J. Electroceram. **4**, 393 (2000).
[3] A. R. James and X. X. Xi, J. Appl. Phys. **92**, 6149 (2002).
[4] B. J. Kennedy and B. A. Hunter, Phys. Rev. B **58**, 653 (1998).
[5] S. P. Alpay and A. L. Roytburd, J. Appl. Phys. **83**, 4714 (1998).
[6] H. Li, W. Si, A. D. West, and X. X. Xi, Appl. Phys. Lett. **73**, 464 (1998).
[7] J. S. Speck and W. Pompe, J. Appl. Phys. **76**, 466 (1994).
[8] J. W. Matthews and A. E. Blakeslee, J. Cryst. Growth **27**, 118 (1974).
[9] K. P. Fahey, B. M. Clemens, and L. A. Wills, Appl. Phys. Lett. **67**, 2480 (1995).
[10] J. C. Jiang, X. Q. Pan, and C. L. Chen, Appl. Phys. Lett. **72**, 909 (1998).
[11] J. C. Jiang, W. Tian, X. Q. Pan, Q. Gan, and C. B. Eom, Appl. Phys. Lett. **72**, 2963 (1998).
[12] J.-P. Maria, H. L. McKinstry, and S. Trolier-McKinstry, Appl. Phys. Lett. **76**, 3382 (2000).
[13] A. E. Romanov, W. Pompe, and J. S. Speck, J. Appl. Phys. **79**, 4037 (1996).
[14] C. L. Canedy, H. Li, S. P. Alpay, L. Salamanca-Riba, A. L. Roytburd, and R. Ramesh, Appl. Phys. Lett. **77**, 1695 (2000).
[15] J. S. Wu, C. L. Jia, K. Urban, J. H. Hao, and X. X. Xi, J. Mater. Res. **16**, 3443 (2001).
[16] E. J. Tarsa, E. A. Hachfeld, F. T. Quinlan, J. S. Speck, and M. Eddy, Appl. Phys. Lett. **68**, 490 (1996).
[17] L. S. J. Peng, X. X. Xi, B. H. Moeckly, and S. P. Alpay, Appl. Phys. Lett. **83**, 4592 (2003).
[18] M. Hiratani, K. Imagawa, and K. Takagi, J. Appl. Phys. **78**, 4258 (1995).
[19] D. Fuchs, M. Adam, P. Schweiss, S. Gerhold, S. Schuppler, R. Schneider, and B. Obst, J. Appl. Phys. **88**, 1844 (2000).